

MR urography: Anatomical and quantitative information on congenital malformations in children

Maria Karaveli, Dimitrios Katsanidis¹, Ioannis Kalaitzoglou², Afroditi Haritanti³, Anastasios Sioundas, Athanasios Dimitriadis³, Kyriakos Psarrakos

Department of Medical Physics, Medical School, Aristotle University of Thessaloniki (AUTH), ¹Pediatric Clinic (AUTH), AHEPA Hospital, ²"Asclepios" Diagnostic Center-MRI, Thessaloniki, ³Department of Radiology (AUTH), AHEPA Hospital, Thessaloniki, Greece

ABSTRACT

Background and Aim: Magnetic resonance urography (MRU) is considered to be the next step in uro-radiology. This technique combines superb anatomical images and functional information in a single test. In this article, we aim to present the topic of MRU in children and how it has been implemented in Northern Greece so far. The purpose of this study is to demonstrate the potential of MRU in clinical practice. We focus both on the anatomical and the quantitative information this technique can offer. **Materials and Methods:** MRU was applied in 25 children (ages from 3 to 11 years) diagnosed with different types of congenital malformations. T₁ and T₂ images were obtained for all patients. Dynamic, contrast-enhanced data were processed and signal intensity versus time curves were created for all patients from regions of interest (ROIs) selected around the kidneys in order to yield quantitative information regarding the kidneys function. **Results:** From the slopes of these curves we were able to evaluate which kidneys were functional and from the corticomedullary cross-over point to determine whether the renal system was obstructed or not. **Conclusion:** In all 25 cases MRU was sufficient, if not superior to other imaging modalities, to establish a complete diagnosis.

Key words: Congenital malformations in children, MR urography, renal MRI

Address for correspondence:

Maria Karaveli,
15th str. N. Redestos, Themi,
Thessaloniki, 57001,
PO Box 2005, Greece.
E-mail : mariakaraveli@yahoo.gr

INTRODUCTION

Magnetic resonance urography (MRU) is considered by many to be the next step in the evolution of uro-radiology in children.¹ MRU combines superb anatomic imaging as well as quantitative evaluation of the urinary system, without the use of ionizing radiation, in a single test.²⁻⁵

The quantitative information provided by MRU imaging is mostly functional information of renal perfusion, excretion, and drainage. However, one of the most significant advantages of this procedure is the acquisition of images with higher contrast, spatial, and temporal resolution in any orthogonal plane compared with conventional techniques.²⁻⁴

During the last 3 years we began applying this technique, in pediatric patients with urological and kidney problems

in northern Greece.⁶ Our goal was to establish a complete protocol for the procedure, which can produce adequate imaging, both static and dynamic. We applied this technique to 25 children diagnosed with different types of congenital malformations.

MRU was proved to be sufficient, if not superior, compared to other imaging modalities.⁷

MATERIALS AND METHODS

All patients, regarding this study, were children (ages from 3 to 11 years). We investigated 25 children, 9 of which were girls (ages 5–10 years) and 16 boys (ages 3–11 years). The parents were informed about the examination procedure and both parents and the children were informed that good cooperation during the acquisition of the breath-hold sequences is very important for the best image quality to be achieved. All children were hydrated prior to the study and remained fasted for 5 hours prior to the examination. No sedation was used⁸ and all patients were asked to void before undergoing the examination.

All patients were placed in a supine position on the scanner bed and scout images were taken in order to determine the accurate position of the kidneys and bladder and to

Access this article online

Quick Response Code:



Website:

www.nigeriamedj.com

DOI:

10.4103/0300-1652.110052

improve, as much as possible, the signal-to-noise ratio for those anatomical structures.⁹

The children were positioned on the table with the head first. The axis of the body coincided with the isocenter of the magnet, with the hands parallel to the body, in order to ensure easier access for the administration of contrast agents.

Patients were instructed to hold their breath during each acquisition and breathe during the intervals between acquisitions. These guidelines helped to reduce motion artifacts otherwise seen in these images.

Furosemide was administered (furosemide, 20 mg/2 ml – LASIX, Sanofi Aventis AEBE) to all patients 15 minutes prior to the examination.

Two types of contrast agents were used: OMNISCAN (287 mg/ml) and MAGNEVIST (469 mg/ml), Gadopentetic acid, Dimeglumine salt with a 0.1 mmol/kg dosage.

The imaging protocol consisted of 2D and 3D acquisitions. The scanner was a GE Signa Infinity HD 1.5T with EXCITE III and upgrade 2007. The chosen flip angle was 90°.

Images were acquired with the following sequences: 2D T2-weighted fat saturation, 3D single shot fast spin-echo (SSFSE/RARE), 2D Radial SSFSE and T1-weighted gradient LAVA (3D SPGR).

Due to MRU's inherent high-contrast and spatial resolution as well as rapid temporal resolution, it is possible to evaluate the signal intensity changes over time, in various regions of the kidney. For this reason, time-signal intensity curves were obtained for all patients by two different ways.

1. Regions of interest (ROIs) were drawn from maximum intensity projections (MIPs) depicting clearly both kidneys after the administration of the contrast agent. In the first case ROIs were drawn around each kidney and the aorta [Figure 1]. Those ROIs acted as a mask on the whole data set of images, for as long as the sequence lasted (5 minutes).
2. ROIs were drawn for the cortex and the medulla of one kidney, along with the aorta. Corresponding ROIs were drawn for the other kidney and aorta [Figure 2]. Those ROIs were in the order of 30 mm².

Additionally, the volume of each kidney was calculated for each patient, using the MRI software. For the volume calculation ROIs were drawn around each kidney for every image of the 3D LAVA sequence [Figure 3]. Then a 3D reconstruction of the kidney was obtained [Figure 4] and the volume was calculated.

The pelvis was excluded from the contour of the kidneys because it was decided that the volume should only include the parenchyma and calyces. The complete protocol is demonstrated in Table 1.



Figure 1: ROIs around each kidney and the aorta

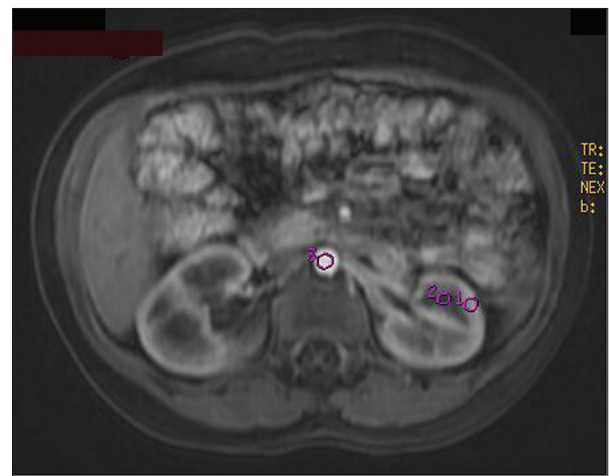


Figure 2: ROIs around the cortex and medulla of left kidney as well as the aorta

RESULTS

Static MRU – T2 sequences

Static-fluid MRU is independent of the renal excretory function and therefore can be used to patients with nonexcreting kidneys.¹⁰ The T2 sequences used in this investigation (thick slab T2 sequences) differentiated between obstructed and nonobstructed ureters. The main advantage of thick slab images was the accurate delineation of nondilated ureters [Figure 5].

Static MRU depends mostly on the existence of urine in the collecting system. Therefore, it is mostly helpful for demonstrating dilated, obstructed, pelvocalyceal systems.⁹ In such cases the thick-slab T2 sequences reveal not only the dilatation but also the point of obstruction [Figure 6].

Normal and abnormal structures filled with fluid restrain MRU, since T2 techniques are not specific for urine but for water. It became apparent that intravenous hydration

Table 1: Suggested MRU protocol

Procedure	Location	Imaging plane	Sequence	TR (msec)	TE (msec)	Matrix	FOV	Slice thickness (mm)
Precontrast imaging	Abdomen + pelvis	3 planes	Localizer	—	—	—	—	—
	Upper pole + bladder	Axial	2D T2-FSE RTr FatSAT	5455	85-95	320×224	48	5/1
	Abdomen + pelvis	Axial	2D T2-FSE RTr FatSAT	5455	85-95	320×224	48	5/1
	Diaphragm up to pelvis	Coronal	3D SS-FSE (MRCP) RTr	3158	335-355	256×128	32-48	1.4/0.7
	Ureters	Radial	2D Thick slab SS-FSE	2319	900	480×256	34	40
Contrast agent administration	Upper pole up to bladder	Coronal	3D LAVA	4.1	2	320×160	34-48	4.4/2.2
		Axial	3D LAVA	4.2	2	320×160	34-48	4.4/2.2
10 minutes after contrast agent administration	Upper pole up to bladder	Coronal	3D LAVA	4.1	2	320×160	34-48	5
		Axial	3D LAVA	4.2	2	320×160	34-48	4.4
		Coronal	3D LAVA	4.2	2	320×160	34-48	4.4

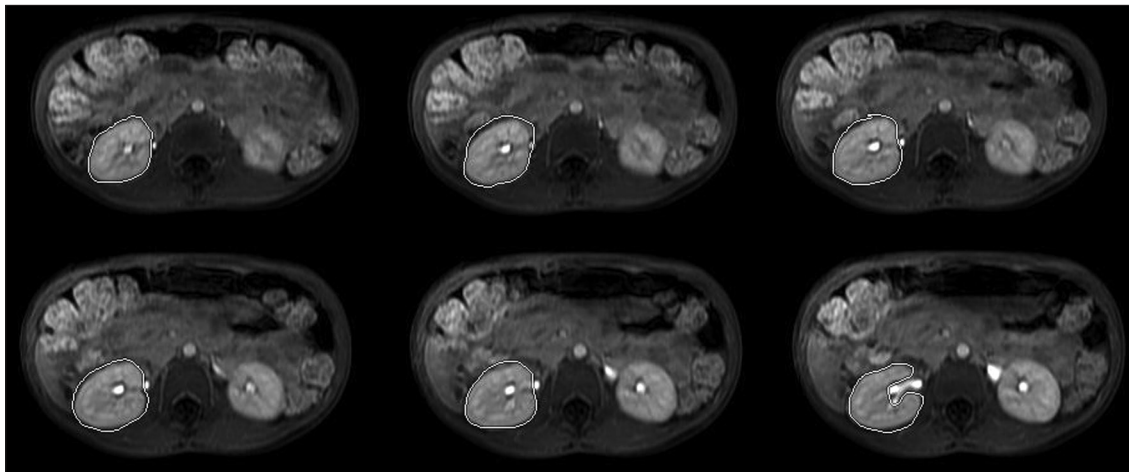


Figure 3: Consecutive images of the contour of a patient's right kidney arising from the 3D LAVA series



Figure 4: The volume of a patient's right kidney in different angles around the axis, for four different positions

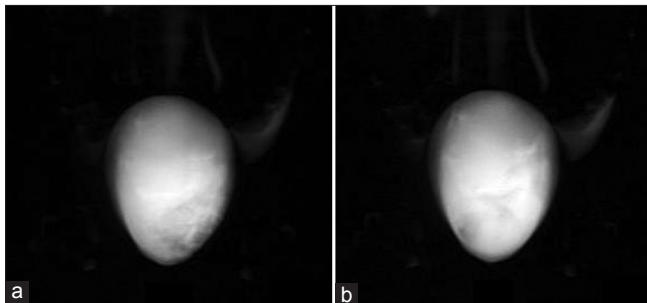


Figure 5: (a) Coronal T2 thick-slab MRU, MRCP ASSET sequence, in a 9-year-old girl with VUR III on the right. The ureters are not displayed properly. (b) Coronal T2 thick-slab MRU from the same series of the MRCP ASSET sequence. Both ureters are depicted accurately

is better compared to oral hydration, before static-fluid MRU, in patients with nondistended ureters because the contrast between the bowel and fluid-filled structures is enhanced.

Excretory MRU – T1 sequences

Excretory MRU using T1 sequences is most helpful for reproducing quantitative results and therefore provide information about the function of the renal system as well as the anatomy.

Signal intensity vs. time curves

As it was mentioned in the method, ROIs were selected, corresponding to the cortex and the medulla of each kidney,

from axial slices of the kidneys, after the administration of contrast agent and signal intensity versus time curves were obtained [Figure 7].

Our results agree with other studies that the cortex demonstrates an initial peak, due to the concentration of the contrast material in the proximal convoluted tubule and a secondary reflecting the concentration of the contrast material in the distal convoluted tubule.¹¹ Then the curve follows the time decay of the contrast agent in the plasma. The medulla curve has a lesser increase in signal intensity and depicts only one delayed peak, corresponding to the entrance of the contrast agent in the loop of Henle.¹

Additionally, ROIs were selected for each kidney (right and left) along with the aorta [Figure 8].

Integrals of the time-intensity curves

Integrals were obtained for all the curves and it was noticed that the addition of the intensity in both kidneys was about 1.5 times higher to the signal from the aorta. This result

could be justified, considering that the clearance of the contrast material from the aorta is quicker compared to the delayed clearance from the kidneys, since they are full of blood vessels and have particular tissue structure.

Slopes of the time-intensity curves

Slopes for each curve were also obtained in the second minute [Figure 9]. The MRI software of the GE Signa Infinity HD 1.5T MRI produced the Y axis results in relative signal intensity. The slope values ranged between 414 and 2376. We observed that for slope values 1000–2000 the kidney was functioning normally. For slope values <1000 and >2000 the kidney was not functioning properly.

The corticomedullary cross-over point

The corticomedullary cross-over point was calculated for all patients. This is the point where the cortex curve intersects with the medulla curve. According to the literature the corticomedullary cross-over point is delayed in obstructed systems, because increased intratubular pressure results in secondarily decreased GFR.¹ In our

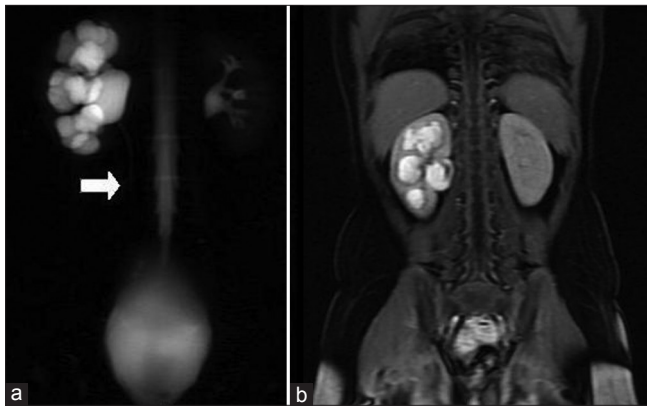


Figure 6: (a) Coronal T2 thick-slab MRU of a 7-year-old girl. The dilatation on the right is visible as well as the point of obstruction (arrow). (b) Coronal MRU with LAVA sequence, after the administration of contrast agent, revealing the dilatation but not the point of obstruction

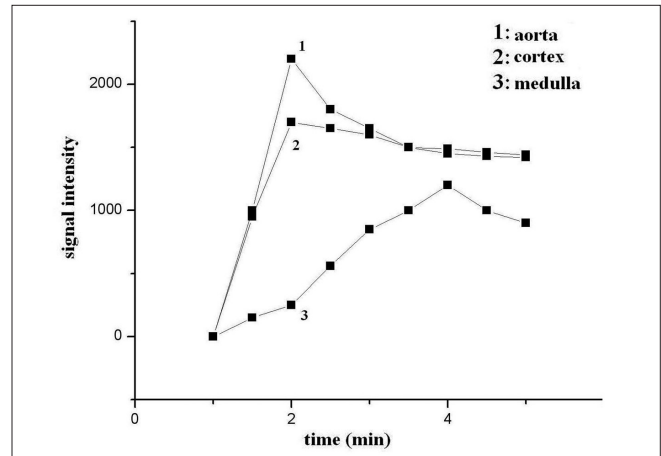


Figure 7: Signal intensity versus time curves for the aorta, cortex and medulla of the right kidney of a healthy patient

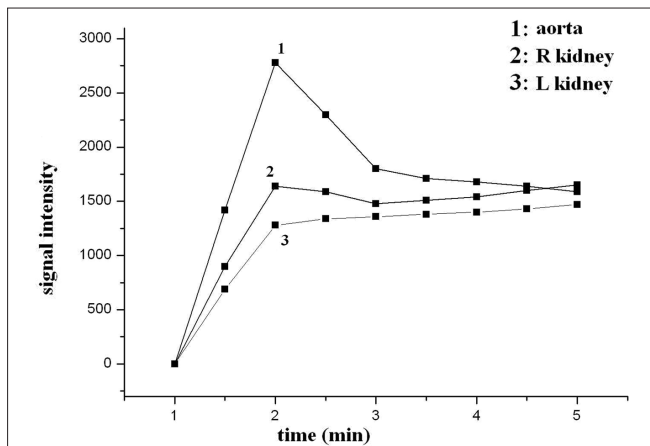


Figure 8: Signal intensity versus time curves for the aorta, right and left kidney of a healthy patient

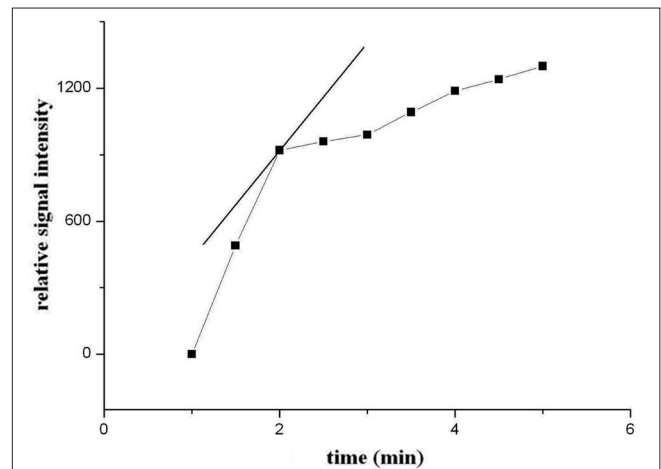


Figure 9: The slope of the curve in the second minute

cases, when the corticomedullary cross-over point was less than 300s the system was not obstructed. For values greater than 300s, 80% of the systems were obstructed.

Split renal function

The split renal function (SRF) is the most widely used parameter of renal function.¹² The SRF was calculated using the following formulas:¹²

SRF of the right kidney = integral of the time-intensity curve of the right kidney × volume of right kidney

SRF of the left kidney = integral of the time-intensity curve of the left kidney × volume of left kidney.

The whole theory of SRF is based on the assumption that voxels represent either functional or nonfunctional tissue. Then if all voxels with a significant signal are summed, the functional volume of each kidney can be calculated. In all of the 25 cases investigated, the calculated SRF agreed with the SRF arising from nuclear medicine studies.

MRU applications in congenital malformations

Our patients were all children, as it was mentioned previously; therefore the clinical entities under investigation were mostly congenital malformations. The MRU anatomic results for the most common congenital malformations are mentioned below.

Hydronephrosis

The most common indication for MRU is the evaluation of hydronephrosis, especially in infants and young children.¹ However, differentiating obstructed from nonobstructed kidneys is almost unrealistic, since most hydronephrotic systems are obstructed to some degree.

From our experience the MRU results coincide with the results from other techniques and modalities like ultrasound, computed tomography, scintigraphy, and/or pyelography. However in 2 out of 9 cases with hydronephrosis, the MRU results overruled the previous diagnosis and revealed the actual pathology. In the first case, concerning a boy diagnosed with bilateral vesicoureteral reflux (VUR), the MRU revealed obstructive uropathy with dilatation of the left ureter, in the upper 2/3 of its length, to the level of the iliac vessels.

In the second case, regarding a 6.5-year-old girl with hydronephrosis on the right, the MAG-3 scan, showed delayed drainage on the right. However, the diuretic scan showed good preservation of the differential function in the kidneys (R=47.4%, L=52.6%) and acceptable washout after LASIX administration, and the delay was characterized as functional. The MRU was requested because an ultrasound check showed that the dilatation of the right pelvic-calyceal system was severe, but there was no dilatation of the right ureter. This finding demonstrated a strong possibility

that the right ureteropelvic junction was obstructed. The MRU revealed, with great sharpness, the existence of ureteropelvic junction obstruction on the right and the child was submitted to pyeloplasty on the right.

From our experience the ureters are reliably identified in most children with MRU.

Renal hypodysplasia

High-resolution anatomic MRU images can reveal anomalous calyceal development, less functioning parenchyma with or without dilated pelvocalyceal systems and cysts, better than any other imaging modality. All those findings indicate anomalous interaction between ureteric bud and the metanephric blastema. Therefore, only one test (MRU) is in most cases sufficient, in identifying renal hypodysplasia.

Fourteen of the children under investigation were diagnosed with renal hypodysplasia, with or without renal scars (12 boys and 2 girls). The cause of renal hypodysplasia in most children (9 out of 12) was congenital VUR [Figure 10].

VUR

Diagnosing VUR can be achieved with other imaging modalities, except MRU. The main advantage of MRU is its ability to reveal other associated congenital anomalies as well as VUR's sequelae, like renal hypodysplasia and renal scars.

Renal ectopia

Renal ectopia can also be diagnosed by other imaging techniques. The high-contrast and high-resolution MRU



Figure 10: 8-year-old boy, with bilateral VUR IV and renal failure since birth. The MRU demonstrated small kidneys bilaterally, the dilatation of the pelvocalyceal system on the left with anomalous calyceal development both left and right. These findings suggest congenital renal abnormalities caused at an initial stage in nephrogenesis. Possibly, an ectopic ureteric orifice caused bilateral VUR and renal hypodysplasia, according to Mackie and Stephens¹³

images, though, provide substantial information about the associated pathology and portray the bigger picture in many cases.

Other congenital malformations

Imaging paraureteral diverticula and renal cysts is superior with MRU, due to its ability to demonstrate with high resolution the anatomic structures. Horseshoe kidneys can be visualized accurately even when atypical types of horseshoe kidneys are not clearly viewed by other modalities and are considered a question mark. We have had two cases with indications of atypical horseshoe kidneys but the proof came only with MRU.

From our experience, we came to the conclusion than all of our cases could be diagnosed only with MRU, because MRU not only demonstrated what we already knew, from past examinations, but also revealed in some cases new clinical findings.

DISCUSSION

Imaging renal structure and function with MRI techniques is not something new. However, the advances in technology provide new tools and strategies to be considered. The properties of T1- and T2-weighted images play a significant part in designing an MRU protocol. We considered all the protocols suggested by the literature and constructed one that seems to produce the basic MRU results for everyday use. In MRU the T1 effects are desirable since they enhance urine. On the other hand T2 effects are not desired since they destroy the contrast between urine and adjacent tissues. Therefore, a good MRU protocol should apply sequences and parameters that reinforce T1 and subdue T2 effects. This can be achieved by implementing a small TE (time-to-echo) and a large flip angle.

T2-weighted images are acquired with long TR and TE. We applied the FSE sequence to produce T2-weighted images and the times used were TR=3158, TE=350 ms. T1-weighted images are acquired with small TR and TE. We applied the LAVA sequence to produce T1-weighted images and the times used were TR=4.1 ms, TE=2 ms. These values were sufficient and produced high-quality T2 and T1 images.

The dosage of the contrast material was 0.1 mmol/kg. There is a lot of debate about the proper amount of contrast material. It is known that the smaller the dosage the more linear the relationship between the concentration of the contrast agent and the signal intensity.¹ Nolte-Ernsting *et al.*¹⁴ suggest 0.05 mmol/kg and Teh *et al.*¹⁵ propose 0.025 mmol/kg. We found that the dosage of 0.1 mmol/kg is sufficient in producing the basic clinical results required by MRU. More sophisticated protocols use lesser contrast agent in order to produce more quantitative results.

Furosemide is a loop diuretic that causes uniform distribution of Gd-DTPA in the urinary tract. We administered Furosemide simultaneously with the administration of Gd-DTPA and in some cases 15 minutes before the administration of Gd-DTPA. We observed that the administration of Furosemide 15 minutes before Gd-DTPA is best because when the contrast agent is administered the Furosemide effect peaks.

The implemented protocol produced signal intensity versus time curves that were responsible for the calculation of many quantitative parameters depicting renal function. There are many parameters that can be calculated with MRU and in most cases require specific protocols. We calculated the SRF which was similar to the radionuclide studies. The corticomedullary cross-over point was investigated. When the corticomedullary cross-over point was less than 300s the system was not obstructed. For values greater than 300s, 80% of the systems were obstructed. Even though the corticomedullary cross-over point is mentioned by many authors no values have been published. Therefore our results cannot be cross-referenced. However, our protocol was limited since the dynamic sequences used were applied for only 5 minutes each. The next step would be to apply the sequences for 10 minutes in order to determine the exact point, if possible, that distinguishes obstructed with nonobstructive systems.

The anatomic images acquired with MRU were superior to those obtained with ultrasonography and scintigraphy. Congenital malformations in children were imaged in great detail and in some cases the MRU images overruled the previous diagnosis based on ultrasound and radionuclide studies.

The main drawback encountered in this study was calming the children in order to tolerate the MRU procedure, because no sedation or anesthesia was used. Especially the younger children required the presence of their mother.

MRU is the next step in the evolution of urology in children and more research needs to be done in order to establish more sophisticated and at the same time easy to implement in everyday use protocols.

REFERENCES

1. Grattan-Smith JD, Jones RA. MR urography in children. *Pediatr Radiol* 2006;36:1119-32.
2. Borthne A, Pierre-Jerome C, Nordshus T, Reisetter T. MR urography in children: current status and future development. *Eur Radiol* 2000;10:503-11.
3. Riccabona M. Pediatric MRU - its potential and its role in the diagnostic work up of upper urinary tract dilatation in infants and children. *World J Urol* 2004;22:79-87.
4. Grattan-Smith JD. MR urography: anatomy and physiology. *Pediatr Radiol* 2008;38(Suppl 2):S275-80.
5. Grattan-Smith JD, Little SB, Jones RA. MR urography in

- children: how we do it. *Pediatr Radiol* 2008;38(Suppl 1): S3-17.
6. Karaveli M, Katsanidis D, Kalaitzoglou I, Haritanti A, Sioundas A, Dimitriadis A, *et al.* The contribution of MR urography in imaging congenital malformations in children – preliminary results. *AUMJ* 2011;38:57-62.
 7. Battal B, Kocaoglu M, Akgun V, Aydur E, Dayanc M, Ilica T. Feasibility of MR urography in patients with urinary diversion. *J Med Imaging Radiat Oncol* 2011;55:542-50.
 8. Borthne A, Nordshus T, Reisetser T, Geitung JT, Gjesdal KI, Babovic A, *et al.* MR urography: the future gold standard in paediatric urogenital imaging? *Pediatr Radiol* 1999; 29: 694- 701.
 9. Jones RA, Perez-Brayfield MR, Kirsch AJ, Grattan-Smith JD. Renal transit time with MR urography in children. *Radiology* 2004;233: 41-50.
 10. Leyendecker JR, Barnes CE, Zagoria RJ. MR urography: Techniques and clinical applications. *Radiographics* 2008;28: 23-48.
 11. Krier JD, Ritman EL, Bajzer Z, Romero JC, Lerman A, Lerman LO. Noninvasive measurement of concurrent single-kidney perfusion, Glomerular filtration and tubular function. *Am J Physiol Renal Physiol* 2001;281:F630-8.
 12. Jones RA, Schmotzer B, Little SB, Grattan-Smith JD. MRU post-processing. *Pediatr Radiol* 2008;38(Suppl 1):S18-27.
 13. Mackie GG, Stephens FD. Duplex kidneys: a correlation of renal dysplasia with position of the ureteral orifice. *J Urol* 1975;114:274-80.
 14. Nolte-Ernsting CCA, Staatz G, Tacke J, Gunter RW. MR urography today. *Abdom Imaging* 2003;28:191-209.
 15. Teh HS, Ang ES, Wong WC, Tan SB, Tan AGS, Chng SM, *et al.* MR renography using a dynamic gradient-echo sequence and low-dose gadopentetate dimeglumine as an alternative to radionuclide renography. *AJR Am J Roentgenol* 2003;181:441- 50.

How to cite this article: Karaveli M, Katsanidis D, Kalaitzoglou I, Haritanti A, Sioundas A, Dimitriadis A, Psarrakos K. MR urography: Anatomical and quantitative information on congenital malformations in children. *Niger Med J* 2013;54:136-42.

Source of Support: Nil, **Conflict of Interest:** None declared.